European Journal of Radiology Open 7 (2020) 100207

Contents lists available at ScienceDirect

European Journal of Radiology Open

journal homepage: www.elsevier.com/locate/ejro

Comparative analysis between synthetic mammography reconstructed from digital breast tomosynthesis and full-field digital mammography for breast cancer detection and visibility

Ryusuke Murakami[a,*], Nachiko Uchiyama[b], Hitomi Tani[a], Tamiko Yoshida[a], Shinichiro Kumita[a]

[a] Department of Radiology, Nippon Medical School Hospital, 1-1-5, Sendagi, Bunkyo-ku, Tokyo, 1138602, Japan
[b] Department of Radiology, National Cancer Center, 5-1-1 Tsukiji, Chuo-ku, Tokyo, 1040045, Japan

ARTICLE INFO

Keywords:
Synthetic mammography
Digital breast tomosynthesis
Digital mammography
Breast cancer
BI-RADS category

ABSTRACT

Purpose: To compare observer performance between synthetic mammography (2DSM) and full-field digital mammography (FFDM) for breast cancer detection and visibility.
Method: A retrospective analysis was conducted on 136 histopathologically proven cases of breast cancer in patients who underwent FFDM and digital breast tomosynthesis (DBT). 2DSM images were reconstructed from DBT data, and 2DSM and FFDM images were reviewed and evaluated for mammographic features, probability of malignancy (BI-RADS classification), and lesion conspicuity. DBT images were not reviewed. Statistical differences in cancer detection rates between 2DSM and FFDM images were analyzed using the McNemar test, agreement on BI-RADS assessment between 2DSM and FFDM was assessed using Cohen's kappa test, and the Wilcoxon's signed rank test was used to compare visibility scores.
Results: Mean cancer detection rates with 2DSM and FFDM images were 84.6 % and 87.8 %, respectively. In subgroup analyses, differences in breast density, tumor size, and presence of calcifications were not statistically significant. Agreement between 2DSM and FFDM images for BI-RADS classification was graded as good with Cohen's k-coefficient of 0.78 ± 0.05. Visibility scores in both modalities of images were similar for all lesions combined; however, 2DSM had significantly better visibility scores for calcified cancers ($p < 0.01$), and in dense breast tissue ($p < 0.01$).
Conclusions: Diagnostic performances of 2DSM and FFDM images were comparable for detecting breast cancers, and it is possible that 2DSM may eliminate the need for additional FFDM during DBT-based imaging due to advances in image reconstruction methods.

1. Introduction

Digital breast tomosynthesis (DBT) has proven to be a promising imaging technology for breast cancer detection [1–4]. It involves obtaining three-dimensional (3D) images of breast tissue by acquiring a series of low-dose projections at different tube positions as the mammography tube rotates along a limited arc around the compressed breast. Using mathematical algorithms, data from these multiple low-dose projections can be reconstructed as a quasi-3D breast volume of thin slices that is parallel to the detector plane. Thus, overlapping breast tissues remain separated and the findings on various planes are more easily seen on the individual slices [5]. When used in population screening, especially in women with dense breasts, DBT has been shown to significantly improve breast cancer detection and reduce recalls compared to conventional mammography [6,7]. Furthermore, multiple population-based studies have shown that a combination of DBT and full-field digital mammography (FFDM) has higher accuracy than digital mammography alone, both for screening and diagnosis settings of breast cancer [3,8–12].

Despite this, the combination of DBT and FFDM has some disadvantages; with the most important being the almost two-fold increase in radiation exposure compared to standard FFDM alone [13,14]. This remains a cause of concern, even though this level is below the average glandular dose limit established by the US Food and Drug Administration (FDA).

Recent technological improvements proposed to resolve this problem include using reconstruction algorithms capable of directly generating 2D synthetic mammography (2DSM) images from the DBT dataset as these reconstructed images do not require additional radiation exposure [13–15]. 2DSM images are generated by summing and

* Corresponding author.
E-mail address: rywakana@nms.ac.jp (R. Murakami).

https://doi.org/10.1016/j.ejro.2019.12.001
Received 21 June 2019; Received in revised form 30 November 2019; Accepted 8 December 2019

filtering the reconstructed DBT sections that produce an image which is similar in appearance to conventional two-dimensional FFDM image.

Some published studies have addressed the clinical performance of 2DSM images, and the initial experience with 2DSM imaging was that it may not be effective [14]. Gur et al. have demonstrated that a combined DBT and 2DSM method had lower sensitivity for cancer detection than a combined DBT and FFDM method; this was mainly attributed to poor quality of the 2DSM images [14]. Currently, advances have significantly improved 2DSM image quality and 2DSM images are now approved for clinical use by the FDA, albeit not approved by all vendors, but only when interpreted in combination with DBT images [16]. Studies using improved 2DSM images have reported that the diagnostic performance of these images was not inferior to that of FFDM images [13,17–20]. Further, it has been reported that the performance of a combination of the current SM and DBT methods is comparable to FFDM and DBT with respect to the screening environment, and is, therefore, adequate for routine clinical use [17,18].

Nevertheless, there is concern that 2DSM is inferior to FFDM as 2DSM is not intended for stand-alone use in clinical practice, either for screening or diagnosis, and because it is only used as a complementary imaging modality along with DBT. Experimental studies directly comparing performance between FFDM and 2DSM images from phantom models show some differences between the two modalities [19,21]. These findings, and consequent assumptions that 2DSM might not be as good as the 'real' 2D images, have not been adequately addressed by clinical studies. Moreover, observer studies have not evaluated the effects of cancer characteristics on the diagnostic performance of 2DSM and FFDM images, even though it is well-known that the size or associated calcification of cancers can influence the diagnostic yield of mammography and that sensitivity is especially low for small, non-calcified cancers [22].

Therefore, we investigated the clinical use of 2DSM imaging by directly comparing breast cancer detection and visibility between 2DSM and FFDM images.

2. Material and methods

2.1. Study design and patient sample

This retrospective study was approved by the institutional ethics committee and used imaging data from consecutive patients who were referred to our institution, a tertiary referral hospital, from April 2017 to March 2018. This data set included patients in whom 2DSM images were obtained, along with at least one detected mammographic abnormality on either FFDM or DBT modalities. Following our institutional protocol, all patients were informed about the procedures and the potential use of their data for research purposes just prior to the assessment, and signed consent forms were obtained. The study conformed to the Helsinki Declaration of 1975 and its subsequent modifications.

Our dataset comprised images from 136 patients with a mean age of 60 (± 11.8) years. These patients were referred to our hospital due to suspicious malignant lesions detected with screening ultrasound or mammography performed at different hospitals for proper management. All lesions of breast cancer in the study cohort were confirmed by surgery, and the final histopathologic results of surgical specimens were used as the standard reference. Cancer incidence in the study population included 112 cases of invasive ductal carcinoma, 16 ductal carcinoma in situ, one invasive lobular carcinoma, and 7 other cancers. To establish reference mammographic findings of the study cohort, two radiologists (R.M and N.U) determined the morphology and visibility of the cancers on 2DSM and FFDM images in consensus. They did not participate in the reading study and were informed of final histological diagnoses and findings with other imaging modalities.

2.2. Image acquisition

DBT and FFDM images were sequentially acquired during one session with single breast positioning and compression per view, while mediolateral oblique and cranio-caudal views were acquired as 25 projections over an angle of 50° (Mammomat Inspiration; Siemens, Erlangen, Germany). An anode/filter combination W/Rh was used at a tube voltage identical to that used for FFDM, along with automated exposure control and iterative reconstruction technique [23]. The DBT slice images were reconstructed as 2-mm thick slices with 1-mm slice distance and a high in-plane resolution of 0.085 mm × 0.085 mm. 2DSM images were created by summing and filtering the stack of reconstructed DBT sections using image processing software (Insight 2D; Siemens, Erlangen, Germany) [23,24].

Average glandular dose (AGD) per exposure as well as breast thickness measured using DBT and FFDM were retrieved from the DICOM headers on the images and were based on automatic exposure settings.

2.3. Observer study

Two dedicated breast radiologists (H.T and T.Y) participated in the observer study. The readers had 7 years of clinical experience with DBT, corresponding to > 600 DBT images per year and 1 year of 2DSM image reading experience. The readers knew that lesions were present in all images but were blinded to type of lesion or its presence in specific images, patient clinical history, and diagnosis. All images were interpreted on a dedicated digital mammography workstation (Plissimo MG, Panasonic, Osaka, Japan) equipped with a set of 5-MP monochrome LCD monitors (MFGD5621HD, 2048 × 2560 pixels, 21.3 inch; BARCO, Torhout, Belgium). Each reader individually analyzed the images in a routine mammography reading room.

2DSM and FFDM images of all patients were divided into two data sets. Initially, FFDM images from group A (68 cases) and 2DSM images from group B (68 cases) were evaluated. Next, SM images from group A and FFDM images from group B were evaluated. Additional images (e.g., magnification views) were not included in the present study. 2DSM and FFDM images were reviewed in random order and were differently sorted. Reviews of the two data sets were spaced 4 weeks apart. DBT slices were not used in this study. To minimize learning bias, reviewers were blinded to patient names, age, and identification number.

The observers scored images based on the following parameters:

1) Morphological features of the detected lesion (mass, focal asymmetry, architectural distortion, and microcalcification).
2) Probability of malignancy for any detected finding (per breast) using the Breast Imaging Reporting and Data System (BI-RADS) assessment categories.
3) Lesion conspicuity evaluated on a four-point visibility scale with 0 = not visible; 1 = low conspicuity and very difficult characterization; 2 = medium conspicuity and difficult characterization; and 3 = high conspicuity and clear characterization.

2.4. Statistical analysis

Final assessments using 2DSM and FFDM were divided into two categories based on BI-RADS score as positive (score of 3–5) or negative (score of 1–2), and true or false interpretations of the observers were assessed in both 2DSM and FFDM images according to the pathologic reference standard and reference mammographic findings. Cancer detection rates (percentage of detected cancers per total cancers) and conspicuity scores of 2DSM and FFDM were also compared. For subgroup analyses, patients were grouped according to breast density (non-dense, n = 52; dense, n = 84), tumor size (≤1 cm, n = 15; 1–2 cm, n = 72; > 2 cm, n = 49), or presence of calcification (calcified cancers,

n = 42; non-calcified, n = 94). Breast density was categorized as either dense breasts, including heterogeneous or extremely dense breasts, or non-dense breasts, including almost fatty or fibro-glandular scattered breasts. Non-calcified cancers included cancers that appeared as a mass, with focal asymmetry, asymmetry, or architectural distortion.

The kappa test was used to assess inter-observer variability in terms of the final assessment (BI-RADS category assignment) and agreement between 2DSM and FFDM images based on mammographic features (calcified and non-calcified cancer) and breast density (dense and non-dense breasts). Degrees of agreement were categorized as follows: k values of 0.00–0.20 indicated poor agreement; 0.21–0.40, fair agreement; 0.41–0.60, moderate agreement; 0.61–0.80, good agreement; and 0.81–1.00, excellent agreement.

Differences in cancer detection rates between 2DSM and FFDM images were analyzed using the McNemar test. Wilcoxon's signed rank test was used to compare visibility scores. These analyses were performed using SAS statistical software (SAS system for Windows, version 9.1.3; SAS Institute, Cary, NC, USA). A p-value < 0.05 was considered statistically significant.

3. Results

The mean cancer detection rate for 2DSM and FFDM images were 84.2 % and 87.8 %, respectively, and the overall diagnostic performance in detecting cancer for 2DSM and FFDM images is presented in Table 1. In subgroup analyses, there was no significant difference between the two observers with respect to breast density, tumor size, and presence of calcifications.

Table 1
Cancer detection rate of 2DSM and FFDM for each observer.

	Cancer detection rate (%)*		
	2DSM	FFDM	p-value
All lesions (n = 136)			
Observer 1	84.6 (115/136)	86.8 (119/136)	0.73
Observer 2	83.8 (114/136)	89.0 (121/136)	0.12
Mean	84.2	87.8	
Breast density			
Non-dense breast (n = 52)			
Observer 1	90.4 (47/52)	94.2 (49/52)	0.47
Observer 2	88.5 (46/52)	96.2 (50/52)	0.13
Mean	89.5	95.2	
Dense breast (n = 84)			
Observer 1	81.0 (68/84)	83.3 (70/84)	0.72
Observer 2	81.0 (68/84)	84.5 (71/84)	0.54
Mean	81.0	83.9	
Tumor size			
Tumor ≤1 cm (n = 15)			
Observer 1	60.0 (9/15)	53.4 (8/15)	0.99
Observer 2	53.4 (8/15)	60.0 (9/15)	0.99
Mean	56.7	56.7	
Tumor 1 – 2 cm (n = 72)			
Observer 1	83.3 (60/72)	87.5 (63/72)	0.37
Observer 2	83.3 (60/72)	90.3 (65/72)	0.13
Mean	83.3	88.9	
Tumor > 2 cm (n = 49)			
Observer 1	93.9 (46/49)	98.0 (48/49)	0.47
Observer 2	98.0 (48/49)	95.9 (47/49)	0.99
Mean	96.0	97.0	
Mammographic features			
Calcified cancers (n = 42)			
Observer 1	92.9 (39/42)	97.6 (41/42)	0.48
Observer 2	92.9 (39/42)	100 (42/42)	0.25
Mean	92.9	98.8	
Non-calcified cancers (n = 94)			
Observer 1	80.9 (76/94)	83.0 (78/94)	0.72
Observer 2	79.8 (75/94)	84.0 (79/94)	0.39
Mean	80.4	83.5	

* Cancer detection rate is defined as the percentage of detected cancers per total cancers (number of cases).

Table 2
BI-RADS category assignment: agreement between 2DSM and FFDM images based on mammographic features and breast density.

	Cohen's kappa (95 % CI)
All lesions (n = 136)	
Observer 1	0.78 (0.68–0.89)
Observer 2	0.71 (0.61–0.83)
Mammographic features	
Calcified lesion (n = 42)	
Observer 1	0.88 (0.80–0.95)
Observer 2	0.81 (0.66–0.95)
Non-calcified lesion (n = 94)	
Observer 1	0.75 (0.62–0.88)
Observer 2	0.69 (0.56–0.82)
Breast density	
Non-dense breast (n = 52)	
Observer 1	0.83 (0.71–0.95)
Observer 2	0.72 (0.53–0.90)
Dense breast (n = 84)	
Observer 1	0.75 (0.60–0.90)
Observer 2	0.69 (0.55–0.84)

Table 3
Visibility scores of 2DSM and FFDM images for each observer.

	Visibility scores		
	2DSM	FFDM	p-value
All lesions (n = 136)			
Observer 1	2.11 ± 1.07	2.03 ± 1.03	0.169
Observer 2	2.12 ± 1.10	2.02 ± 1.04	0.086
Mean	2.11 ± 1.05	2.02 ± 1.02	0.093
Breast density			
Non-dense breast (n = 52)			
Observer 1	2.37 ± 0.93	2.44 ± 0.90	0.088
Observer 2	2.35 ± 0.86	2.33 ± 0.90	0.735
Mean	2.36 ± 0.88	2.39 ± 0.88	0.441
Dense breast (n = 84)			
Observer 1	1.95 ± 1.13	1.77 ± 1.08	0.045*
Observer 2	1.98 ± 1.12	1.82 ± 1.03	0.038*
Mean	1.96 ± 1.12	1.80 ± 1.04	0.035*
Tumor size			
Tumor ≤1 cm (n = 15)			
Observer 1	1.27 ± 1.23	1.20 ± 1.27	0.715
Observer 2	1.27 ± 1.34	1.13 ± 1.19	0.753
Mean	1.27 ± 1.24	1.17 ± 1.21	0.866
Tumor 1 – 2 cm (n = 72)			
Observer 1	1.97 ± 1.10	1.96 ± 1.94	0.976
Observer 2	1.92 ± 1.14	2.00 ± 0.99	0.387
Mean	1.94 ± 1.09	1.98 ± 0,99	0.621
Tumor > 2 cm (n = 49)			
Observer 1	2.31 ± 0.90	2.39 ± 0.76	0.458
Observer 2	2.20 ± 0.98	2.39 ± 0.81	0.108
Mean	2.24 ± 0.89	2.38 ± 0.78	0.195
Mammographic features			
Calcified cancers (n = 42)			
Observer 1	2.60 ± 0.73	2.21 ± 0.84	< 0.01*
Observer 2	2.57 ± 0.77	2.24 ± 0.79	< 0.01*
Mean	2.58 ± 0.72	2.23 ± 0.79	< 0.01*
Non-calcified cancers (n = 94)			
Observer 1	1.89 ± 1.13	1.95 ± 1.10	0.276
Observer 2	1.92 ± 1.12	1.92 ± 1.16	0.876
Mean	1.90 ± 1.12	1.93 ± 1.10	0.255

Visibility score data represent mean ± standard deviation (median).

Inter-observer agreement for 2DSM and FFDM images was found to be excellent for BI-RADS classification (Cohen's k-coefficient = 0.84 ± 0.04 and 0.93 ± 0.02, respectively). The agreement in BI-RADS category assignment between 2DSM and FFDM images, determined by Cohen's k-coefficient, is detailed in Table 2. For observer 1, Cohen's k-coefficients for all lesions, calcified cancer, and non-calcified cancer were 0.78 ± 0.05, 0.88 ± 0.04, and 0.75 ± 0.07, while those

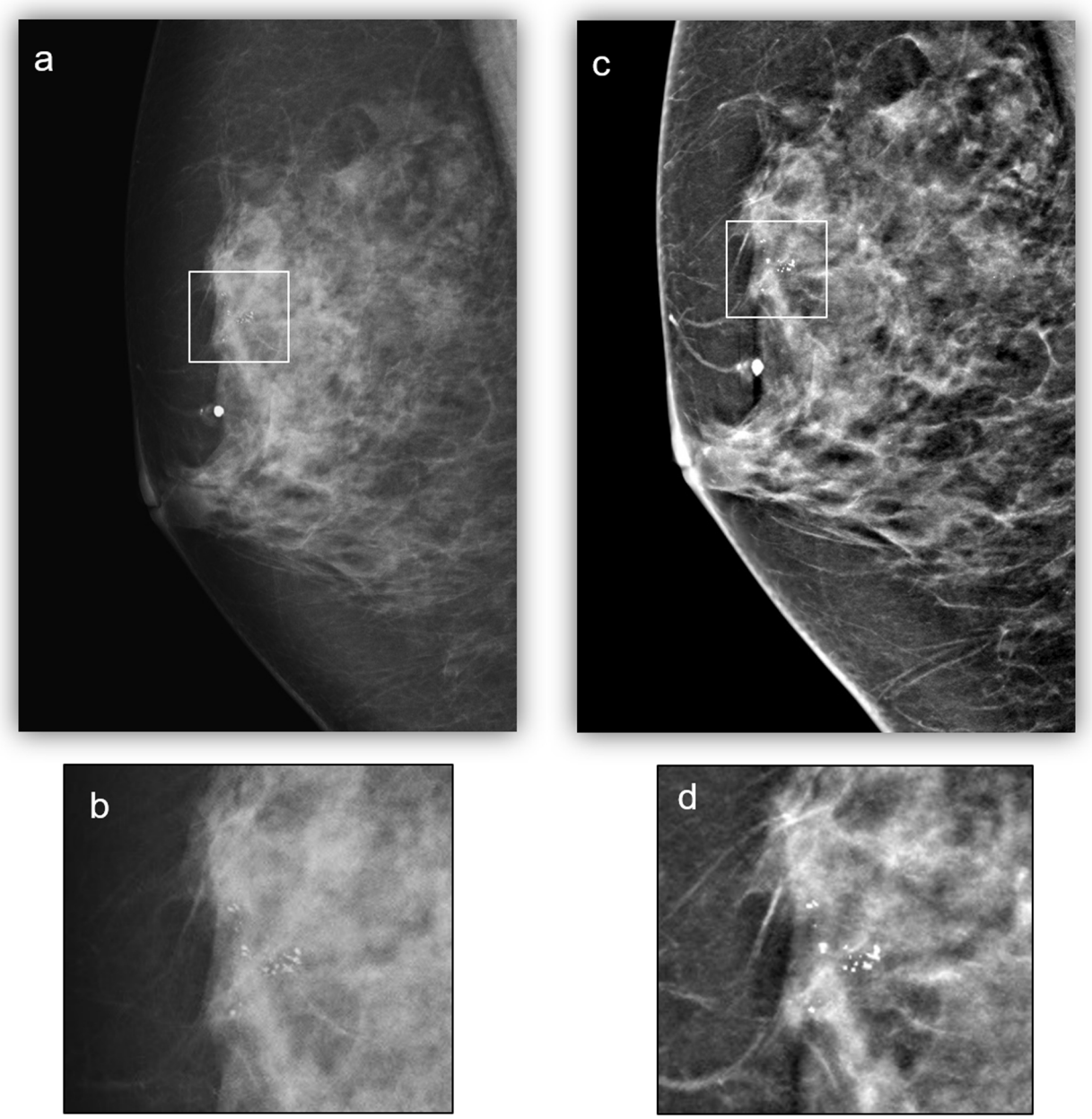

Fig. 1. A 55-year-old woman with microcalcifications in the right breast with biopsy-proven invasive ductal cancer. a) 2DSM, b) Enlarged view of microcalcifications on 2DSM, c) FFDM, d) Enlarged view of microcalcifications on FFDM. Detailed right mediolateral oblique views show that 2DSM better highlights the lesion.

for observer 2 were 0.72 ± 0.06, 0.81 ± 0.08, and 0.69 ± 0.07, respectively.

Visuality scores assigned to 2DSM and FFDM were similar for all lesions (Table 3). However, for visibility scores in non-dense breast, 2DSM and FFDM were 2.11 ± 1.05 and 2.02 ± 1.02 ($p = 0.093$), while those in dense breast 2DSM and FFDM were 1.96 ± 1.12 and 1.80 ± 1.04 ($p = 0.035$), respectively. On mammographic features, for calcified cancers, 2DSM and FFDM were 2.58 ± 0.72 and 2.23 ± 0.79 ($p < 0.01$), while those for non-calcified cancers 2DSM and FFDM were 1.90 ± 1.12 and 1.93 ± 1.10 ($p = 0.255$), respectively. 2DSM was superior to FFDM for calcified lesions ($p < 0.01$) (Fig. 1) and in dense breast tissue ($p < 0.05$) (Fig. 2); these differences were statistically significant.

Mean AGD per view for FFDM was 1.15 mGy (SD 0.49), whereas it was 1.67 mGy (0.63) for DBT and 2.82 mGy (1.10) from dual-acquisition mammography (FFDM plus DBT).

4. Discussion

In most studies, DBT has been used in combination with FFDM, as a double acquisition method. In contrast, synthesized 2D images can be reconstructed from DBT images acquired at an acceptable radiation dose that is in line with the European Guidelines for Quality Assurance in Breast Screening [25]. Our study focused on direct comparison between 2DSM and FFDM images, using an image dataset from 136 patients with histopathologically proven breast cancer and imaging abnormalities. This data set allowed detailed evaluation of these two modalities with respect to detecting and characterizing various types of breast lesions.

Our results show that the clinical performance of 2DSM images, even without DBT information, was not inferior to that of FFDM images in terms of detectability, probability of malignancy, or lesion conspicuity. Although some published studies have compared the clinical performance of 2DSM with DBT and that of FFDM with DBT, the use of

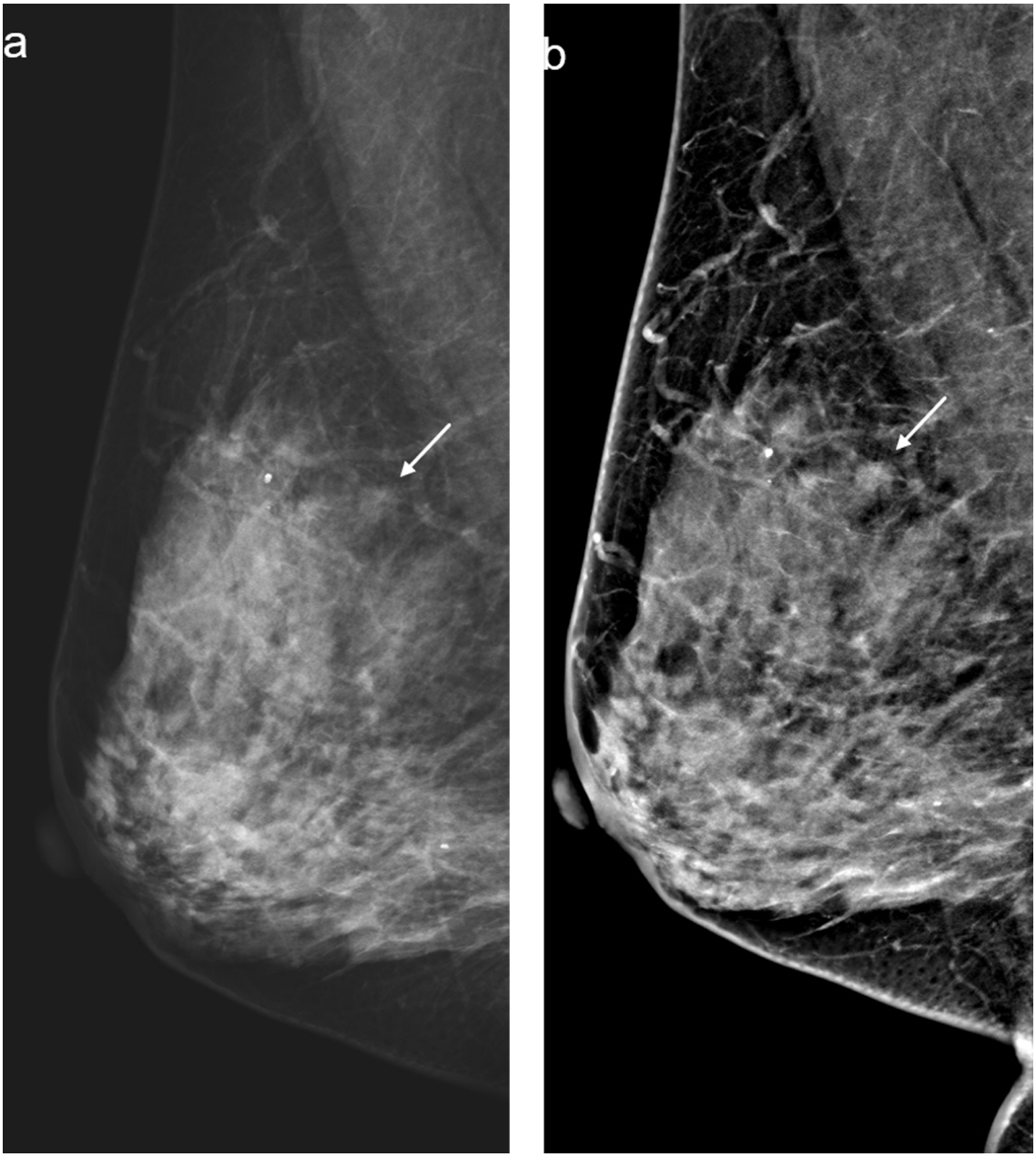

Fig. 2. A 45-year-old woman with invasive ductal cancer (10 mm) and extremely dense breast: a) Mediolateral oblique 2DSM and b) FFDM images demonstrate a mass in the right upper breast. 2DSM better accentuates the lesion compared to FFDM.

2DSM as a valid imaging modality that can replace FFDM in DBT assessments is still being debated [17,26,27]. Additionally, the combination of DBT and FFDM has the disadvantages of longer time for interpretation and higher dose of radiation.

In this study, the BI-RADS category assignment based on 2DSM and FFDM images showed overall good agreement with similar interpretations for tumor size and mammographic findings. Zuley et al. have directly compared 2DSM and FFDM in terms of probability of malignancy assigned to various radiological findings, and they reported that both image types were comparable in performance [13]. Choi et al. have also found no difference in observer sensitivity between 2DSM and FFDM images for the detection of T1-stage invasive breast cancer [20]. Our study supports these findings in that we found no significant difference in breast cancer detection rates between 2DSM and FFDM images.

Lesion visibility evaluation showed significant differences between the two imaging modalities, and it was dependent on the type of mammographic features and breast density. These results can be attributed to differences in image impressions of microcalcifications between 2DSM and FFDM. Depending on the image reconstruction algorithms used in 2DSM, and in comparison with FFDM, in some cases, images were depicted as having variations in density patterns in the masses and in background breast densities, apart from differences in density and morphology of the microcalcifications. These differences have been reported by other studies on phantom models [19,21]. In 2DSM, the ability to discriminate can be affected by the structure of the reconstruction algorithm itself. Nelson et al., in their in vitro evaluation, have suggested that 2DSM images demonstrated a visual enhancement of larger microcalcifications [21]. However, it is possible that structural background noise, which plays an important role in lesion identification, cannot be exactly reproduced in an in vitro environment.

Interpretation of microcalcifications using DBT remains debated. Theoretically, a single DBT slice image may show only a few calcifications of a clinically significant microcalcification cluster, and this can

negatively affect the radiologists' perception. On the other hand, FFDM can effectively detect calcifications because its high contrast resolution has been tailored to reveal calcifications [27,28]. Some studies have shown that, compared to DBT alone, FFDM has higher sensitivity in detecting and characterizing calcifications [29]. Given the above, we performed subgroup analysis based on the presence of calcification. Visibility scores of calcified cancer in SM images were significantly higher than those in FFDM images, suggesting that SM may compensate for the drawbacks of DBT, i.e., underestimation of calcification. However, our study is limited by the fact that the number of calcified lesions was low (n = 42). Therefore, future studies with a large number of calcified lesions are needed to verify the suitability of 2DSM images.

In dense breasts, cancer detection rate using 2DSM images was similar to that with FFDM images, and this result concurs with those reported by previous studies. However, visibility scores were significantly higher in 2DSM images than in FFDM images. In dense breasts, FFDM could not overcome limitations of mammography, such as normal overlapping tissues of various densities, textures mimicking suspicious asymmetries, and dense breast tissue obscuring non-calcified lesions. It is possible that 2DSM has the advantage of using images less affected by tissue overlapping in DBT than FFDM; consequently, our results suggest that 2DSM may reduce unnecessary imaging or biopsies without loss in sensitivity in patients with dense breast tissues who need to undergo DBT-based imaging.

Our study has a few limitations. First, this is a retrospective single-center study that included a series comprising malignant cases enriched with abnormalities. Thus, it may not be representative of the general population undergoing screening and our results may not be broadly transferable to other settings. Additionally, imaging was performed in machines supplied by a single vendor (Siemens), and a multi-institutional trial with multiple radiologists, with varying levels of experience, and various imaging vendors are needed to validate our findings. Finally, it should be noted that this comparison of 2DSM with FFDM does not mean that we advocate the use of 2DSM alone. 2DSM remains complementary to DBT acquisition and is to be used in combination with DBT images during clinical decision-making.

In conclusion, the results of this direct comparison of the two 2D breast imaging modalities confirms a promising role for SM as an alternative to FFDM. 2DSM can provide equal and, in some cases, even superior diagnostic performance, with the added advantage of requiring lower dose exposure. 2DSM images are currently not intended to be used as a stand-alone diagnostic 2D imaging modality, or should only be used as a guide during interpretation of DBT. Our findings further support the fact that DBT can be used, either in clinical or screening environments, as a primary imaging modality, and that it can be complemented by 2DSM without the need for FFDM.

Declaration of Competing Interest

All authors have no conflicts of interest and no disclosures of financial interest to report.

Acknowledgments

This work was supported by Japan Society for the Promotion of Science Grant Number JP17K10375. We would like to thank Editage (www.editage.jp) for English language editing.

References

[1] N. Houssami, P. Skaane, Overview of the evidence on digital breast tomosynthesis in breast cancer detection, Breast 22 (2013) 101–108, https://doi.org/10.1016/j.breast.2013.01.017.

[2] S. Ciatto, N. Houssami, D. Bernardi, F. Caumo, M. Pellegrini, S. Brunelli, P. Tuttobene, P. Bricolo, C. Fanto`, M. Valentini, S. Montemezzi, P. Macaskill, Integration of 3D digital mammography with tomosynthesis for population breast-cancer, Lancet Oncol. 14 (2013) 583–589, https://doi.org/10.1016/S1470-2045(13)70134-7.

[3] P. Skaane, A.I. Bandos, R. Gullien, E.B. Eben, U. Ekseth, U. Haakenaasen, M. Izadi, I.N. Jebsen, G. Jahr, M. Krager, L.T. Niklason, S. Hofvind, D. Gur, Comparison of digital mammography alone and digital mammography plus tomosynthesis in a population-base screening program, Radiology 267 (2013) 47–56, https://doi.org/10.1148/radiol.12121373.

[4] S.M. Friedewald, E.A. Rafferty, S.L. Rose, M.A. Durand, D.M. Plecha, J.S. Greenberg, M.K. Hayes, D.S. Copit, K.L. Carlson, T.M. Cink, L.D. Barke, L.N. Greer, D.P. Miller, E.F. Conant, Breast Cancer screening using tomosynthesis in combination with digital mammography, JAMA 311 (2014) 2499–2507, https://doi.org/10.1001/jama.2014.6095.

[5] I. Sechopoulos, A review of breast tomosynthesis: part I: the image acquisition process, Med. Phys. 40 (2013) 014301, , https://doi.org/10.1118/1.4770279.

[6] N. Houssami, R.M. Turner, Rapid review: estimates of incremental breast cancer detection from tomosynthesis (3D mammography) screening in women with dense breasts, Breast 30 (2016) 141–145, https://doi.org/10.1016/j.breast.2016.09.008.

[7] E.A. Rafferty, M.A. Durand, E.F. Conant, D.S. Copit, S.M. Friedewald, D.M. Plecha, D.P. Miller, Breast cancer screening using tomosynthesis and digital mammography in dense and nondense breasts, JAMA 315 (2016) 1784–1786, https://doi.org/10.1001/jama.2016.1708.

[8] P. Skaane, R. Gullien, H. Bjørndal, E.B. Eben, U. Ekseth, U. Haakenaasen, G. Jahr, I.N. Jebsen, M. Krager, Digital breast tomosynthesis (DBT): initial experience in a clinical setting, Acta Radiol. 53 (2012) 524–529, https://doi.org/10.1258/ar.2012.120062.

[9] E.A. Rafferty, J.M. Park, L.E. Philpotts, S.P. Poplack, J.H. Sumkin, E.F. Halpern, L.T. Niklason, Assessing radiologist performance using combined digital mammography and breast tomosynthesis compared with digital mammography alone: results of a multicenter, multireader trial, Radiology 266 (2013) 104–113, https://doi.org/10.1148/radiol.12120674.

[10] D. Gur, A.I. Bandos, H.E. Rockette, M.L. Zuley, J.H. Sumkin, D.M. Chough, C.M. Hakim, Localized detection and classification of abnormalities on FFDM and tomosynthesis examinations rated under an FROC paradigm, AJR Am. J. Roentgenol. 196 (2011) 737–741, https://doi.org/10.2214/AJR.10.4760.

[11] G. Gennaro, A. Toledano, C. di Maggio, E. Baldan, E. Bezzon, M. La Grassa, L. Pescarini, I. Polico, A. Proietti, A. Toffoli, P.C. Muzzio, Digital breast tomosynthesis versus digital mammography: a clinical performance study, Eur. Radiol. 20 (2010) 1545–1553, https://doi.org/10.1007/s00330-009-1699-5.

[12] S. Ciatto, N. Houssami, D. Bernardi, F. Caumo, M. Pellegrini, S. Brunelli, P. Tuttobene, P. Bricolo, C. Fantò, M. Valentini, S. Montemezzi, P. Macaskill, Integration of 3D digital mammography with tomosynthesis for population breast cancer screening (STORM): a prospective comparison study, Lancet Oncol. 14 (2013) 583–589, https://doi.org/10.1016/S1470-2045(13)70134-7.

[13] M.L. Zuley, B. Guo, V.J. Catullo, D.M. Chough, A.E. Kelly, A.H. Lu, G.Y. Rathfon, M. Lee Spangler, J.H. Sumkin, L.P. Wallace, A.I. Bandos, Comparison of two dimensional synthesized mammograms versus original digital mammograms alone and in combination with tomosynthesis images, Radiology 271 (2014) 664–671, https://doi.org/10.1148/radiol.13131530.

[14] D. Gur, M.L. Zuley, M.I. Anello, G.Y. Rathfon, D.M. Chough, M.A. Ganott, C.M. Hakim, L. Wallace, A. Lu, A.I. Bandos, Dose reduction in digital breast tomosynthesis (DBT) screening using synthetically reconstructed projection images; an observer performance study, Acad. Radiol. 19 (2012) 166–171, https://doi.org/10.1016/j.acra.2011.10.003.

[15] Ruth C, Smith A, Stein J, System and method for generating a 2D image from a tomosynthesis data set. US Patent 7,760,924, 2010.

[16] U.S. Food and Drug Administration, Meeting of the Radiological Devices Advisory Panel, (2017) P080003/S001 Hologic Selenia dimensions 3D System, FDA Executive Summary, Published October 24. (Accessed January 2017) http://www.fda.gov/downloads/advisoryCommittees/CommitteesMeetingMaterials/MedicalDevices/MedicalDevicesAdvisoryCommittee/RadiologicalDevices-Panel/UCM324861.pdf.

[17] P. Skaane, A.I. Bandos, E.B. Eben, I.N. Jebsen, M. Krager, U. Haakenaasen, U. Ekseth, M. Izadi, S. Hofvind, R. Gullien, Two-view digital breast tomosynthesis screening with synthetically reconstructed projection images: comparison with digital breast tomosynthesis with full field digital mammographic images, Radiology 271 (2014) 655–663, https://doi.org/10.1148/radiol.13131391.

[18] D. Bernardi, P. Macaskill, M. Pellegrini, M. Valentini, C. Fanto`, L. Ostillio, P. Tuttobene, A. Luparia, N. Houssami, Breast cancer screening with tomosynthesis (3D mammography) with acquired or synthetical 2D mammography compared with 2D mammography alone (STORM-2): a population- based prospective study, Lancet Oncol. 17 (2016) 1105–1113, https://doi.org/10.1016/S1470-2045(16)30101-2.

[19] S. Peters, M. Hellmich, A. Stork, J. Kemper, O. Grinstein, M. Pu¨sken, L. Stahlhut, S. Kinner, D. Maintz, K.B. Krug, Comparison of the detection rate of simulated microcalcifications in full-field digital mammography, digital breast tomosynthesis, and synthetically reconstructed 2-dimensional images performed with 2 different digital X-ray mammography systems, Invest. Radiol. 52 (2017) 206–215, https://doi.org/10.1097/RLI.0000000000000334.

[20] J. Choi, B.K. Han, E.Y. Ko, E.S. Ko, S.Y. Hahn, J.H. Shin, M.J. Kim, Comparison between two-dimensional synthetic mammography reconstructed from digital breast tomosynthesis and full-field digital mammography for the detection of T1 breast cancer, Eur. Radiol. 26 (2016) 2538–2546, https://doi.org/10.1007/s00330-015-4083-7.

[21] J.S. Nelson, J.R. Wells, J.A. Baker, E. Samei, How does c-view image quality compare with conventional 2D FFDM? Med. Phys. 43 (2016) 2538–2547, https://doi.org/10.1118/1.4947293.

[22] W.A. Berg, Z. Zhang, D. Lehrer, R.A. Jong, E.D. Pisano, R.G. Barr, M. Böhm-Vélez, M.C. Mahoney, W.P. Evans 3rd, L.H. Larsen, M.J. Morton, E.B. Mendelson,

D.M. Farria, J.B. Cormack, H.S. Marques, A. Adams, N.M. Yeh, G. Gabrielli, ACRIN 6666 Investigators, Detection of breast cancer with addition of annual screening ultrasound or a single screening MRI to mammography in women with elevated breast cancer risk, JAMA 307 (2012) 1394–1404, https://doi.org/10.1001/jama.2012.388.

[23] S. Abdurahman, F. Dennerlein, A. Jerebko, A. Fieselmann, T. Mertelmeier, Optimizing high resolution reconstruction in digital breast tomosynthesis using filtered back projection, Lect. Notes Comput. Sci. (Including Subser. Lect. Notes Artif. Intell. Lect. Notes Bioinformatics), Springer International Publishing, Switzerland, 2014, pp. 520–527, https://doi.org/10.1007/978-3-319-07887-8_73.

[24] F. Dennerlein, A. Jerebko, A. Fieselmann, T. Mertelmeier, Efficient synthesis of virtual projections from a tomosynthesis data set using a 2D image processing method, Proc. SPIE 8668 (2013), https://doi.org/10.1117/12.2008011 86680W1-8.

[25] N. Perry, M. Broeders, C. de Wolf, S. Törnberg, R. Holland, L. von Karsa, European guidelines for quality assurance in breast cancer screening and diagnosis. Fourth edition–summary document, Ann. Oncol. 19 (2008) 614–622, https://doi.org/10.1093/annonc/mdm481.

[26] F. Gilbert, L. Tucker, M.G. Gillan, P. Willsher, J. Cooke, K.A. Duncan, M.J. Michell, H.M. Dobson, Y.Y. Lim, T. Suaris, S.M. Astley, O. Morrish, K.C. Young, S.W. Duffy, Accuracy of digital breast tomosynthesis for depicting breast cancer subgroups in a UK retrospective reading study (TOMMY Trial), Radiology 277 (2015) 697–706, https://doi.org/10.1148/radiol.2015142566.

[27] M.L. Spangler, M.L. Zuley, J.H. Sumkin, G. Abrams, M.A. Ganott, C. Hakim, R. Perrin, D.M. Chough, R. Shah, D. Gur, Detection and classification of calcifications on digital breast tomosynthesis and 2D digital mammography: a comparison, AJR Am. J. Roentgenol. 196 (2011) 320–324, https://doi.org/10.2214/AJR.10.4656.

[28] E.F. Conant, Clinical implementation of digital breast tomosynthesis, Radiol. Clin. N. Am. 52 (2014) 499–518, https://doi.org/10.1016/j.rcl.2013.11.013.

[29] A. Tagliafico, G. Mariscotti, M. Durando, C. Stevanin, G. Tagliafico, L. Martino, B. Bignotti, M. Calabrese, N. Houssami, Characterisation of microcalcification clusters on 2D digital mammography (FFDM) and digital breast tomosynthesis (DBT): does DBT underestimate microcalcification clusters? Results of a multicentre study, Eur. Radiol. 25 (2015) 9–14, https://doi.org/10.1007/s00330-014-3402-8.